

How much aromatic naphthalene and graphene are?

Yashita Y. Singh,^a and Vaibhav A. Dixit^{*b}

^aDepartment of Pharmaceutical Chemistry, School of Pharmacy & Technology Management, Shri Vile Parle Kelavani Mandal's (SVKM's), Narsee Monjee Institute of Management Studies (NMIMS), Mukesh Patel Technology Park, Babulde, Bank of Tapi River, Mumbai-Agra Road, Shirpur, Dist. Dhule 425405 India.

^bDepartment of Pharmacy, Birla Institute of Technology and Sciences Pilani (BITS-Pilani), VidyaVihar Campus, street number 41, Pilani, 333031, Rajasthan. India.

Phone No. +91 1596 255652, Mob. No. +91-7709129400,
Corresponding author: Vaibhav A. Dixit

Corresponding author email: vaibhavadixit@gmail.com, vaibhav.dixit@pilani.bits-pilani.ac.in

Abstract

Naphthalene, (Aromatic stabilization Energy; ASE, 50-60 kcal/mol) polyacenes and graphene are considered aromatic. Existing models for polyacenes predict a linearly increasing ASE and give little insights into their high reactivity and decreasing stability. Graphene's aromaticity has been studied earlier qualitatively suggesting alternate Clar's sextet and two-electrons per ring, but ASE estimates have not been reported yet. In this paper, various Heat of Hydrogenation (HoH) and isodesmic schemes have been proposed and compared for the estimation of naphthalene ASE. Results show that HoH schemes are simple to design, are equivalent to isodesmic schemes, and unconjugated unsaturated reference systems predict ASE values in agreement with literature reports. Partially aromatic reference systems underestimate ASE. HoH schemes require calculations for a smaller number of structures, and offer scope for experimental validation, and involve enthalpy differences. Polyacene (X-axis extensions of benzene) ASE estimates (using HoH scheme) correlate well with experimental instability data and offer new physical insights explaining the absence of arbitrarily larger polyacenes. ASEs extrapolated from quadratic and logarithmic regression models have been used to estimate the largest polyacene with limiting ASE values. ASE values for Pyrene (Y-axis extension of benzene) and higher analogues (here called pyrene-vertacenes) are estimated using HoH schemes. Further truncated graphene models and graphene are approximated as combinations of polyacene and pyrene-vertacene units. First ever ASE and molecular sizes (22-255 nM) estimates predict nanometer size ranges for flat graphene in agreement with recent experiments and offer new physical insights. These ASE and size estimates for graphene may prove useful in the design of novel energy (hydrogen) storage, electronic and material science applications.

Keywords

Aromatic stabilization energy, naphthalene, polyacenes, heat of hydrogenation, isodesmic reactions, and graphene.

1 INTRODUCTION

The concepts of aromatic compounds and aromaticity are of paramount importance in chemical research. According to Google Scholar: 1,290,000 and 88,400 articles have been published which contain the terms 'aromatic compounds' and 'aromaticity'. This highlights the significance of and interest in these concepts. Figure 1 shows a historical data on the number of articles published in this area. Since the discovery of benzene the term "aromatic compound" soon began to appear in the scientific literature, but the concept of "aromaticity" emerged ~40 years later (Figure 1) as more compounds with similar features were isolated or made. After World-War II both concepts received an increased interest from the chemical and other scientific communities.

Erich Hückel (in 1938) successfully used quantum mechanics to formulate the criteria for classifying aromatic and non-aromatic compounds.¹ This criteria known as Hückel's rule, states that a compound is aromatic only if it contains $(4n + 2)$ π electrons in a conjugated ring system, where n is a positive integer.² In 1964, Clar proposed Clar's sextet rule which states that in polycyclic aromatic hydrocarbons (PAH), the resonance structure with the highest number of aromatic sextets, is the most important structure contributing to the properties of the molecule.³ The concept of π electron delocalization as a major factor responsible for aromatic properties of compounds like benzene has been questioned and the role of C-C σ bond framework in forcing a symmetrical structure and the π electron delocalization has been put forward by Sason Shaik and other groups.⁴

Contrary to the other key chemical concepts, e.g. nucleophilicity, electronegativity, Lewis acidity/basicity, van der Waals radii, redox-potential; 'aromaticity' is not an observable quantity and thus cannot be precisely measured.^{5,6,7,8,9} As a result, aromaticity is always defined in reference to a non-aromatic compound or a system.¹⁰ For benzene, the difference in the expected Heat of Hydrogenation (HoH) of hypothetical cyclohexatriene (derived from the HoH for cyclohexene,) and the experimental HoH of benzene can be approximated as Aromatic Stabilization Energy (ASE, Equation 1 and Equation 2).

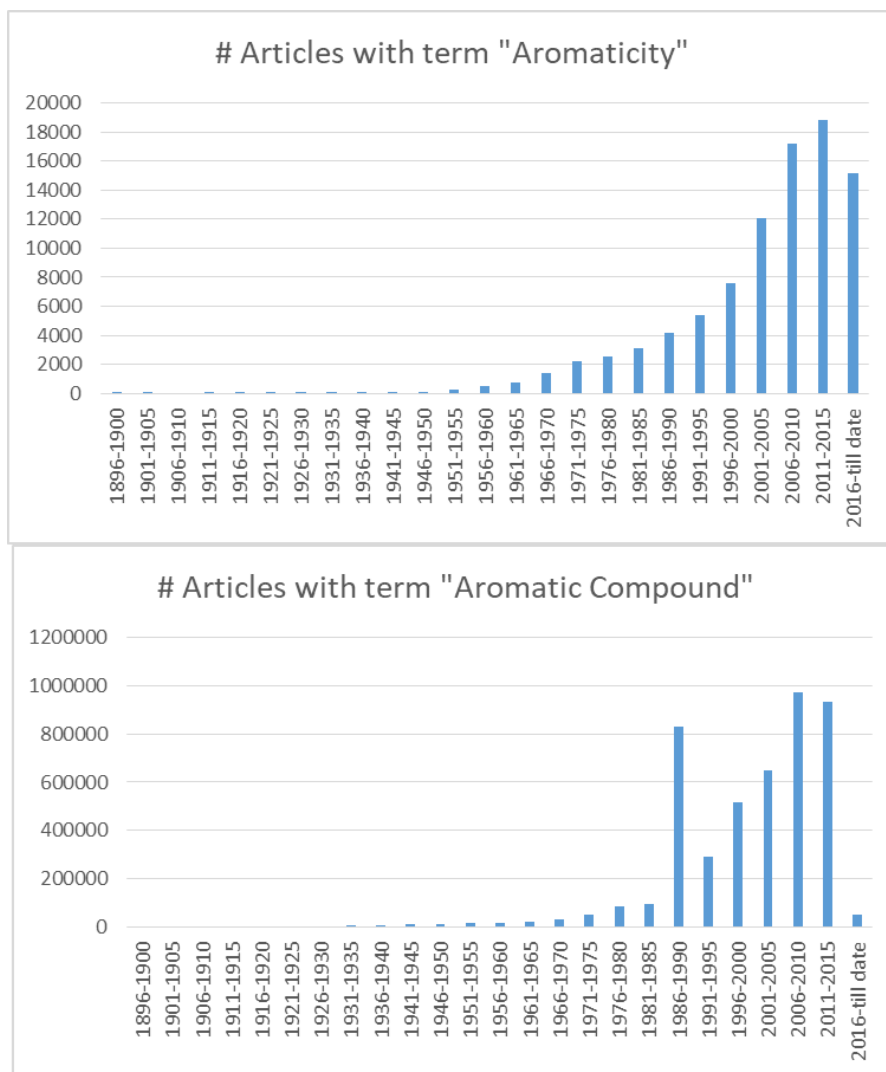
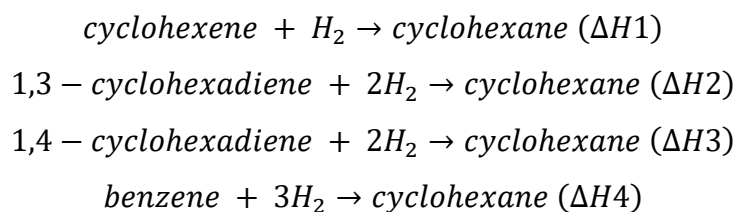


Figure 1. Number of papers, containing the concept of “aromatic compounds” and “aromaticity”, published since the discovery of benzene.

Alternatively, HoH for cyclohexatriene can be estimated from the HoH for 1,3-cyclohexadiene or 1,4-cyclohexadiene as shown in Equation 1 and Equation 2.



Equation 1. The heat of hydrogenation for cyclohexene, cyclohexadienes, and benzene.

Aromatic stabilization energy (ASE) for benzene is then estimated using following equations.

$$ASE1 = 3 * (\Delta H1) - (\Delta H4)$$

$$ASE2 = 3/2 * (\Delta H2) - (\Delta H4)$$

$$ASE3 = 3/2 * (\Delta H3) - (\Delta H4)$$

Equation 2. Aromatic stabilization energy (ASE) for benzene using heats of hydrogenation for cyclohexene, cyclohexadienes, benzenes and the hypothetical cyclohexatriene.

Beckhaus et al. have suggested an ASE value of -35.7 kcal/mol using ASE1 in Equation 2.¹¹ Using Mallon et al.'s HoH value for 1,3-cyclohexadiene (-53.63 kcal/mol), we get ASE2 = -31.35 kcal/mol.¹² For 1,4-cyclohexadiene, Roth et al. have reported HoH = -55.69 kcal/mol and using it as a reference gives an ASE3 of -34.43 kcal/mol.¹³ This suggests that using unconjugated unsaturated systems gives values in close agreement with those estimated from mono-cycloalkenes. Thus unconjugated unsaturated systems are more suitable for the estimation of ASE (via HOHs) since they lack partial stabilization present in conjugated reference compounds.

Many indices and measures have been proposed in the past for estimating relative aromaticity and are discussed in detail in excellent reviews elsewhere.^{6,8-10,14-16} Briefly, most of the geometric parameters depend on the fact that carbon-carbon bond lengths in aromatic compounds are intermediate between those of singly and doubly bonded carbons. Amongst the geometric indices developed till date, Harmonic Oscillator Model of Aromaticity (HOMA), is considered most suitable for predicting aromaticity of many hydrocarbon cycles, and heterocycles.^{5,16,17} Applying the HOMA parameter and its variants for estimating relative aromaticity of PAH presents some difficulties. Multiple HOMA values for each ring are often quoted in the literature and may depend on the theory and basis set used.¹⁵ Magnetic criteria in the form of NMR chemical shifts, magnetic susceptibility exaltation, cyclic current density analysis and nucleus-independent chemical shift (NICS), have been used to gain insights into the aromaticity of a variety of compounds.^{14,7}

The concept of aromaticity has been used in explaining the physical, chemical and recently biological properties of many compounds and materials. Many protein structures are stabilized via aromatic π – cation interactions.^{18,19} Recent findings have shown that modified carbon nanotubes (hydroxyl and amino substituted) adsorb organic

environmental pollutants and may help in pollution control.²⁰ Relative contents of aromatic compounds like naphthalenes, phenanthrenes, and dibenzothiophenes are used as maturity indicators in sedimentary rocks and crude oils.²¹ A variety of aromaticity descriptors have been applied in drug design to enhance the drug-like properties (ligand efficiency and optimize ADMET properties) of small organic compounds.²² Aromaticity indices have also been used as molecular descriptors for prediction of optical properties of 9,10- Anthraquinone derivatives in ethanol solution.²³ Additionally, a new domain in aromaticity research has emerged from recent findings of aromatic compounds in the interstellar medium. Combinations of laboratory spectroscopy and radio astronomy are being used in the detection of these compounds.²⁴ The existence (or viability) of some aromatic compounds and the absence of others, can be linked to the structure, reactivity, stability, and aromaticity in these systems in free space, which can be deduced from calculated or experimental ASEs. Thus quantifying aromaticity especially for larger PAH is vital in getting deeper insights into such problems and applications.

Naphthalene has diverse applications ranging from pharmaceutical industry to material sciences. It is mainly used as a precursor to synthesize other molecules and is a well-known household fumigant. Naphthalene diimide based polymer acceptor in solar cells deliver high performance owing to the electron transportability.²⁵ Naphthalene is toxic and may cause acute hemolytic anemia.²⁶ Naphthalene is reported to have a larger total aromatic stabilization than benzene but is considered less aromatic than benzene with respect to aromatic stabilization per ring (Naphthalene ASE = 51-60 < 2 * 36 kcal/mol). Varying Naphthalene ASE estimates are given in the literature using different computational methods.^{7,10,27,28} The consensus ASE value for benzene (~36 kcal/mol from both experimental and theoretical methods) is well known in the literature, but naphthalene ASE value is debatable and awaits further experimental validation. Schleyer and Pühlhofer have made recommendations for the estimation of ASEs for benzene and naphthalene derivatives.²⁸ They also proposed a hierarchy of homodesmotic reactions for better prediction of thermochemical properties while accounting of various atom, bond, and hybridization types, and minimizing complexity in the reference systems.^{29,30} Even though calculation of ASE of naphthalene has been

attempted, only a limited number of isodesmic schemes have been tested so far (Figure 2).³¹ Considering the better performance of unconjugated reference system for benzene shown above, differences in ring size and strain, these schemes are probably not the best choice. Naphthalene ASE estimates based on number of ring π electrons are in close agreement with calculations (ASE/ π -electron ≈ 6 ; Benzene $6 * 6 = 36$, naphthalene $6 * 10 = 60$ kcal/mol).



Figure 2. Isodesmic schemes for the estimation of ASE of acenes reported by Schleyer et al.³¹ For naphthalene $n = 5$.

Anthracene is also known to follow similar trends in aromatic stabilization i.e. calculated ASE value estimates are less than those extrapolated from the number of fused benzene rings and in better agreement with values based on per electron contributions.⁵ Experimental studies on higher analogs of benzene; like tetracene, pentacene, hexacene and heptacenes show that these are unstable and require special conditions (low-temperature matrix isolation) or derivatization for stabilization and isolation.^{32–34,31} For larger polyacenes trends in ASE have not been studied in depth but various estimates up to heptacene show (in disagreement with experiments) increasing ASE values and aromaticity.^{5,27} Thus physical chemical (especially thermochemical) insights into the quantitative trends in aromaticity for polyacenes are missing in the literature.

Graphene (a fused 2D polymer of benzene), on the other hand, is relatively stable, has unique physical and chemical properties. Its isolation as the 2D material was awarded physics Nobel prize in 2010, triggered an extensive interest and research in this technology sphere.^{35,36,37,38,39,40,41,42} In these works, the importance of graphene aromaticity in determining bandgap, polarizability, optoelectrical, conductivity, electron confinement and other properties resonates. Graphene-based nanotechnology has also been extensively tested for diagnosis, therapeutic and targeted drug delivery applications.²⁶ Many groups have explored the aromatic character of graphene and truncated graphene models, mostly suggesting that two sets of Clar's sextets can be overlaid to explain its aromaticity.^{41,40} Each benzene ring in graphene has been

proposed to retain two electrons thus satisfying Hückel's rule of aromaticity ($n = 0$).³⁹ Thus the aromatic character in graphene is not yet completely understood. Most of these studies attempt to understand and extrapolate aromaticity of graphene qualitatively using electronic, magnetic or geometrical properties (cited above) and estimates of graphene ASE, thermochemical insights into its stability and reactivity are missing in the literature. Structural studies have found that graphene sheets are not perfectly flat, have corrugations and tend to fold or bend beyond a few hundred nanometers.^{43,44} Most of the studies cited above don't directly explain this fact. Graphene and metal-graphene complexes have been studied for their hydrogen storage capacity and as potential energy storage materials.⁴⁵ Formation of hydrogenated graphene (graphane) and its potential for energy storage and electro-optical applications has been reported.⁴⁶ Estimates of ASE for graphene, truncated graphene models and derivatized or doped graphene may prove valuable in the prediction of stability, viability and design of novel graphene-based materials for technological and energy (hydrogen) storage applications.

In this paper, aromatic stabilization energy (ASE) of naphthalene has been estimated using two methods i) Heat of Hydrogenation (HoH) schemes and ii) Isodesmic schemes. Estimated ASE values are then compared and different levels of theory are evaluated for accuracy. The best suitable scheme is then applied for estimating the ASE of polyacenes, Y-axis extensions of benzene (here called pyrene-vertacenes) and small truncated graphene models. Using these findings potential ASE and size estimates for planar graphene are presented and discussed.

2. METHODOLOGY

The structures were drawn using ChemAxon's MarvinSketch 18.3.0 and mol files were converted into GAMESS^{47,48} inputs using wxMacMolPlt.⁴⁹ Quantum chemical calculations involving geometry optimization and vibrational frequency analysis were performed on these structures using HF and DFT (B3LYP functional) level and different basis sets 6-31G(d), 6-311+G(d,p), TZV. High-level G3MP2 and CCSDT calculations were also performed to assess the accuracy of different methods. For larger polyacenes and pyrene-vertacenes (Figure 4 and Figure 5), their partially saturated and

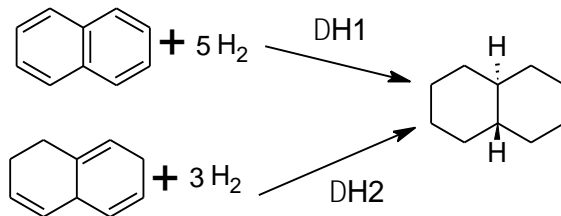
fully saturated analogues, calculations were performed at the HF/6-31G(d) level since it was the least demanding method and showed an excellent correlation with the CCSDT data for naphthalene ASE schemes. All structures were confirmed as ground states (no negative vibrational frequencies) by performing Hessian (frequency) calculations at the end of geometry optimization steps in GAMESS. All trans configurations were used for all partially unsaturated and fully saturated structures used for estimating ASE values. Highest possible symmetry point group was used during all calculations used for ASE estimations of polyacenes, pyrene-vertacenes and truncated graphene models. The energies were modified using zero-point corrections scaled by factors of 0.9135, and 0.9806 for HF and DFT calculations respectively.^{50,51} Recent studies on coronenes have shown that HF and DFT methods are able to predict correct geometry and frequencies for PAH containing up to 54 carbon atoms.⁵² The largest polyacene (dodecacene) studied in this work has 50 carbons, while the largest pyrene-vertacene has 56 carbon atoms. Although for some calculations reported in this work, low positive frequencies were observed, none of the structures gave negative frequencies when using highest symmetry point group.

3. Results and Discussions

The ASE in naphthalene, in spite of containing two fused benzene rings, is not twice that of benzene. Different estimates for ASE (50-60 kcal/mol) based on isodesmic reactions, group additivity concepts exist in the literature and scarcity of thermochemical data for validation has been cited as a major hurdle.^{5,53,27} The heat of Hydrogenation (HoH) has been used historically to estimate Benzene's ASE and also appears in textbook descriptions of its aromaticity.^{5,54} In spite of the conceptual simplicity, lack of conjugational effects (especially in unconjugated reference systems e.g. ASE3 in Equation 2), possible cancellation of any correlational effects, computational advantage over isodesmic schemes, and most importantly possibility for experimental validation, HoH schemes have remained neglected for naphthalene and higher PAH ASE estimations. In the following subsections, different HoH and isodesmic schemes for naphthalene ASE estimation are proposed and compared.

3.1. Heat of Hydrogenation (HoH) schemes for Naphthalene ASE estimation.

The heat of Hydrogenation (HoH) is the enthalpy of hydrogenation reaction for alkenes. According to this scheme, HoH for a hypothetical unconjugated cyclohexatriene is extrapolated from corresponding HoH of unsaturated non-aromatic compounds like cyclohexene, or 1,3-cyclohexadiene. As mentioned in the introduction benzene ASE value derived from 1,4-cyclohexadiene closely agree with a value derived from cyclohexene. Thus all possibilities for mono, di, tri, and tetra-unsaturated decaline reference systems were considered for naphthalene ASE estimation. This helped in analyzing the effect of different types of reference system on the ASE values predicted using HoH schemes shown in Table 1. Figure 3 shows a representative HoH scheme 16, used for naphthalene ASE prediction.



$$\text{Naphthalene ASE} = (5/3 * \text{DH2}) - \text{DH1}$$

Figure 3. A representative HoH scheme 16 used for estimating ASE value for naphthalene.

ASE values predicted with mono-unsaturated reference systems are between -50 and -82 (average across all methods: -65.17) kcal/mol. For di, tri and tetra-unsaturated reference systems the values are -25-74 (average -61.70), -29-70 (average -55.81) and -29-62 (average -41.53) kcal/mol respectively. Moreover the tri-unsaturated and unconjugated reference systems shown in rows 15, 16, and 17 of Table 1, gave ASE values of -54.74, -63.32, and -61.70 kcal/mol respectively at HF/6-31G(d) level. The average for tri-unsaturated unconjugated schemes (59.91 kcal/mol) is in excellent agreement with average at CCSDT level (-59.35 kcal/mol), per π electron estimates, and with literature values reported earlier. In comparison the average ASE estimates at HF/6-31G(d) level for partially conjugated tri-unsaturated schemes 11, 12, 13 and 14 are about 3 kcal/mol higher than at CCSDT level (51.83 kcal/mol) and in disagreement from the widely accepted 60 kcal/mol. This suggests that the tri-unsaturated unconjugated reference systems are the best for estimating naphthalene ASE. Average ASE values for different type of reference systems at each level are given in the Table S3 (see supporting information word file). As the schemes 10, 23 and 24 in Table 1 for tri and tetra-unsaturated reference systems, containing aromatic benzene rings, gave unusually low ASE values, these were excluded from this analysis. Thus partially aromatic reference systems are not suitable for estimation of ASE values in PAH.

3.2. Isodesmic schemes for Naphthalene ASE estimation.

As mentioned in the introduction isodesmic schemes have been used earlier for estimating the ASE of benzene, naphthalene and other polyacenes. Most of these methods used monocyclic reference systems and thus may give less accurate predictions especially for PAH beyond naphthalene. Isodesmic scheme for naphthalene

($n = 5$) shown in Figure 2 predicts an ASE values of 65.74 kcal/mol at HF/6-31G(d) level. While the ASE value predicted using unconjugated reference system (1,4-cyclohexadiene) and similar isodesmic equation (60.48 kcal/mol), not considered by Schleyer^{31,55}, is in close agreement with HoH schemes using unconjugated unsaturated systems. This again highlights the benefit of using unconjugated unsaturated reference systems.

Although for benzene there are only three possible set of reference systems (one mono and two di-unsaturated), for naphthalene and larger PAH the number of different but almost equivalent reference systems increases rapidly. Thus the effect of the type of reference system on the predicted ASE values was analyzed for naphthalene using isodesmic schemes shown in Table 2.

A careful analysis of the data at HF/6-31G(d), which has excellent correlation with CCSDT values, shows that partially aromatic reference systems (schemes 11, 12 and 13 in Table 2), give poor estimates of ASE (average -25.47 kcal/mol). While conjugated reference systems (schemes 4, 5, 6; average ASE = -56.38 kcal/mol, and 14, 15, 16; average ASE = -56.54 kcal/mol) give descent estimates of ASE. Schemes 7, 8, 9 and 10 containing a mix of conjugated and unconjugated systems give better estimates of naphthalene ASE. Schemes 17, 18, and 19 containing all unconjugated systems also give estimates of ASE in close agreement with HoH schemes (Table 2).

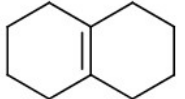
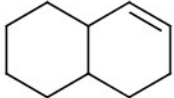
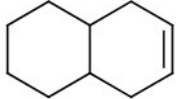
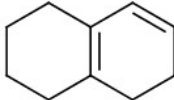
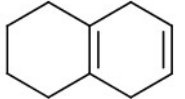
3.3. Comparison of different Naphthalene ASE estimates

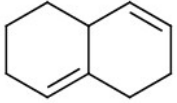
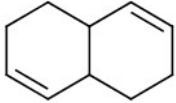
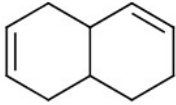

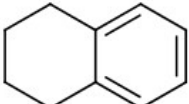
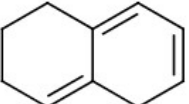
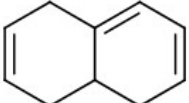
Analysis of the ASE values derived using HoH and isodesmic schemes shows that partially aromatic reference systems are not suitable for estimating aromaticity of naphthalene (and possibly other PAH). Average values for the mono, di, tri and tetra-unsaturated systems show that HoH and isodesmic schemes are almost equivalent to each other. The unconjugated reference systems consistently give values in close agreement with that of literature reports. HoH schemes have some advantages especially relevant to larger PAH. For example to estimate ASE using the unconjugated reference system (HoH scheme 15) optimization and frequency calculations for only three hydrocarbons (the unsaturated reference system, naphthalene, and decalene) are required (excluding the computationally inexpensive dihydrogen). Whereas with

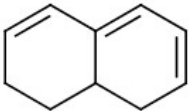
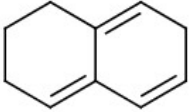
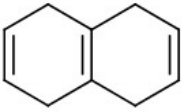
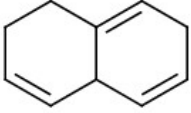
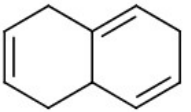
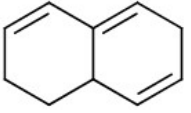
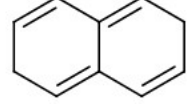
isodesmic schemes, using equivalent unconjugated reference system, calculations on five hydrocarbons are required. For anthracene, and tetracene a similar isodesmic scheme will require calculations for 5, and 6 hydrocarbon structures, while using HoH scheme of similar accuracy calculations for only 3 structures are required (each with 14 and 18 carbons respectively). Thus isodesmic schemes are computationally expensive for ASE estimation especially for larger PAH.

Additionally, isodesmic schemes give ASE as enthalpies of hypothetical reactions and hence are less likely to be verified experimentally. Moreover designing isodesmic schemes for higher PAH is non-trivial considering the large number of possible combination of possible reference structures with close agreement between predicted ASE values. Additionally, isodesmic schemes have been shown to incur errors, especially while modeling thermochemical properties for larger hydrocarbons.⁵⁶ To estimate accurate enthalpies for such reactions requires computationally expensive treatment of electron-electron correlations. ASE estimates from HoH schemes, which are easy to design, require calculations on only 3 hydrocarbon structures, involve differences of enthalpy for two reactions (Equation 1 and Equation 2), and may lead to cancellation of electron-correlation errors. Thus for estimating ASE values for larger PAH, HoH schemes become the obvious preferred choice.

Table 1. Naphthalene aromatic stabilization energies (ASE) obtained from HoH schemes and corresponding reference unsaturated compounds (at HF-TZV, DFT-B3LYP/TZV, G3MP2 and CCSDT levels).

S.No	Reference unsaturated compound	ASE based on HoH schemes				
		HF/6-31G(d)	HF/TZV	B3LYP/TZV	CCSDT	G3MP2
1		-50.81	-54.86	-54.32	-52.33	-58.26
2		-78.84	-80.25	-81.77	-72.84	-72.11
3		-66.35	-66.93	-68.97	-63.96	-63.12
4		-54.64	-56.53	-54.95	-53.02	-54.34
5		-53.08	-55.60	-56.00	-54.60	-55.12

6		-62.45	-64.23	-65.59	-60.38	-61.29
7		-67.80	-69.05	-71.54	-64.68	-64.03
8		-66.46	-67.28	-69.98	-63.58	-62.83
9		-68.23	-68.91	-70.25	-66.23	-65.55
10		-2.07	-1.60	-2.30	-2.32	-3.43
11		-52.71	-54.59	-51.91	-49.72	-50.72
12		-66.42	-67.33	-66.70	-63.35	-63.06

13		-53.85	-55.30	-52.72	-49.68	-49.59
14		-45.89	-48.55	-46.60	-44.59	-44.68
15		-54.72	-56.93	-57.99	-56.24	-55.10
16		-63.32	-65.01	-66.60	-61.52	-61.20
17		-61.70	-63.36	-65.18	-60.28	-59.94
18		-55.44	-57.45	-57.67	-53.62	-53.37
19		-44.48	-47.30	-45.23	-43.65	-42.47

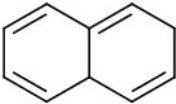
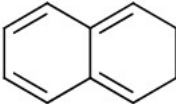
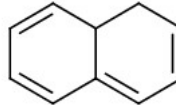
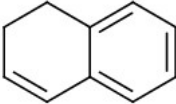
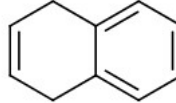
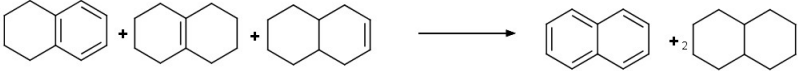
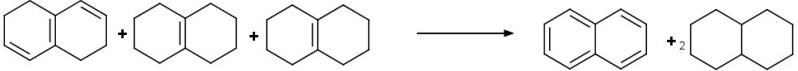
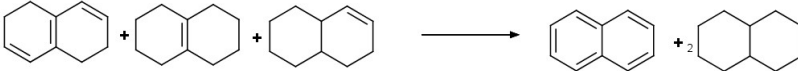
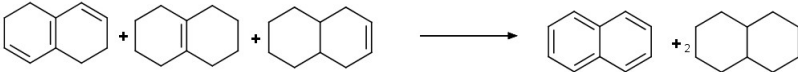

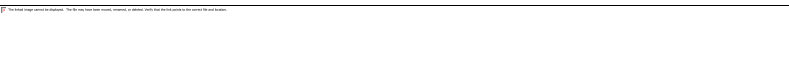

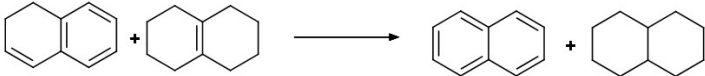
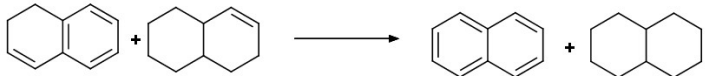
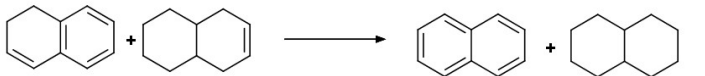
20		-59.07	-60.53	-59.13	-55.41	-54.85
21		-47.11	-48.84	-44.38	-42.91	-42.48
22		-55.27	-56.44	-52.87	-50.54	-49.84
23		-13.52	-13.64	-13.81	-12.83	-13.28
24		-16.63	-16.75	-17.69	-17.46	-17.07

Table 2. Isodesmic schemes and corresponding aromatic stabilization energies obtained at HF-TZV, B3LYP/TZV, CCSDT, G3MP2 level.

S. No.	Isodesmic schemes	HF-TZV	B3LYP/TZV	CCSDT	G3MP2
1	5	-66.93	-68.97	-63.96	-63.12
2	5	-80.25	-81.77	-72.84	-72.11
3	5	-54.86	-54.32	-52.33	-58.26
4	2	-58.61	-57.75	-55.21	-56.09
5	2	-61.27	-60.31	-56.99	-57.89

6	$2 \text{ } \langle \text{Chemical Structure 1} \rangle + \langle \text{Chemical Structure 2} \rangle \longrightarrow \langle \text{Chemical Structure 3} \rangle + 2 \langle \text{Chemical Structure 4} \rangle$	-56.19	-54.82	-52.89	-55.12
7	$\langle \text{Chemical Structure 1} \rangle + \langle \text{Chemical Structure 2} \rangle + \langle \text{Chemical Structure 3} \rangle \longrightarrow \langle \text{Chemical Structure 4} \rangle + 2 \langle \text{Chemical Structure 5} \rangle$	-60.90	-60.73	-57.62	-58.21
8	$\langle \text{Chemical Structure 1} \rangle + \langle \text{Chemical Structure 2} \rangle + \langle \text{Chemical Structure 3} \rangle \longrightarrow \langle \text{Chemical Structure 4} \rangle + 2 \langle \text{Chemical Structure 5} \rangle$	-65.37	-65.38	-61.09	-61.79
9	$\langle \text{Chemical Structure 1} \rangle + \langle \text{Chemical Structure 2} \rangle + \langle \text{Chemical Structure 3} \rangle \longrightarrow \langle \text{Chemical Structure 4} \rangle + 2 \langle \text{Chemical Structure 5} \rangle$	-65.57	-66.33	-61.21	-61.29
10	$\langle \text{Chemical Structure 1} \rangle + \langle \text{Chemical Structure 2} \rangle + \langle \text{Chemical Structure 3} \rangle \longrightarrow \langle \text{Chemical Structure 4} \rangle + 2 \langle \text{Chemical Structure 5} \rangle$	-66.22	-66.43	-62.27	-62.38
11	$\langle \text{Chemical Structure 1} \rangle + \langle \text{Chemical Structure 2} \rangle + \langle \text{Chemical Structure 3} \rangle \longrightarrow \langle \text{Chemical Structure 4} \rangle + 2 \langle \text{Chemical Structure 5} \rangle$	-22.90	-23.11	-22.33	-25.37
12	$\langle \text{Chemical Structure 1} \rangle + \langle \text{Chemical Structure 2} \rangle + \langle \text{Chemical Structure 3} \rangle \longrightarrow \langle \text{Chemical Structure 4} \rangle + 2 \langle \text{Chemical Structure 5} \rangle$	-27.98	-28.60	-26.43	-28.14

13		-25.32	-26.04	-24.65	-26.34
14		-56.77	-54.65	-52.81	-55.22
15		-61.85	-60.14	-56.91	-57.99
16		-59.19	-57.58	-55.14	-56.19
17		-65.08	-65.77	-63.35	-63.51
18		-58.51	-59.45	-57.00	-57.33
19		-56.10	-56.52	-54.68	-56.37

20		-21.88	-21.91	-20.73	-22.27
21		-26.96	-27.40	-24.83	-25.04
22		-24.30	-24.84	-23.06	-23.24

3.4. ASE in polyacenes, and Y-axis extensions of benzene (vertacenes),

Graphene can be thought of as a benzene extended in both X and Y directions to give the well-known two-dimensional honeycomb structure (Figure 4 and Figure 5).³⁹ But the trends in ASE of benzene homologous series on the X-axis i.e. naphthalene (50-60), anthracene (~80), tetracene (naphthacene), pentacene and higher polyacenes are still debated in the literature and not clearly understood. Additionally it is not clear whether the ASE per π electron remains the same, increases or decreases as one moves from benzene, naphthalene, to pyrene and to higher analogs formed from the addition of benzene units on the Y-axis (here called vertacenes Figure 5).

Naphthalene ASE analysis discussed above showed that HF/6-31G(d) method has excellent correlations ($r = 0.996, 0.994$, Table S1) with B3LYP/TZV and high accuracy CCSDT/6-31G(d) methods respectively. Thus, in this study HF/6-31G(d) level calculations were performed to estimate ASE values of PAH larger than naphthalene. Although isodesmic schemes with unconjugated reference systems give ASE estimates in close agreement with literature reports, it is non-trivial to find the best isodesmic schemes for anthracene and higher polyacenes. This is due to larger combinatorial possibilities of equivalent unconjugated reference systems. Thus isodesmic schemes (similar to those used here for naphthalene) are not suitable for estimating ASE of larger polyacenes and vertacenes. Isodesmic schemes for polyacene ASE estimation proposed by Schelyer (Figure 2) uses conjugated 1,3-cyclohexadiene reference system and does not account for strain induced by different number of fused rings. ASE (resonance energy) values reported using this scheme increase linearly ($y = -23.579x - 11.129$, $x = \#$ of rings, $R^2 = 0.9991$, $n = 7$) with the polyacene size and are not in agreement with experimental instability of such systems towards addition reactions.^{31,32,33}

HoH schemes, on the other hand, represent a relatively better choice for estimation of ASE for polyacenes. As seen in Table 1, the unconjugated reference system with maximum double bonds (three for naphthalene) is one of the best choices for estimating ASE. Within such reference systems, scheme 15, with double bonds between the fused carbons and at the periphery is the best choice. Schemes similar to 15 are easy to

design for higher polyacenes. Additionally these systems retain high (C_{2H}) symmetry thus reduce ring, angle strain, do not contain chiral centers (thus avoiding cis-trans effects) and offer scope to estimate ASE for larger polyacenes due to increased computational speed.

Figure 4 shows the structures of polyacenes up to dodecacene for which ASE values were predicted with HoH schemes. ASE values predicted using HoH schemes at HF/6-31G(d) level are shown in Table 3. The ASE value predicted for benzene is in excellent agreement with the experimental value extrapolated using HoH scheme, Equation 1 and Equation 2. Naphthalene ASE value is also in close agreement with the literature values.³¹ Residuals for the quadratic regression model (Table 3) for ASE prediction are within expected experimental errors. Using HoH schemes and the quadratic model for anthracene onwards predict significantly lower ASE values than those reported by Schleyer et al. and other references. Thus HoH schemes predict ASE values in line with experimental findings, offer physical and thermochemical insights into polyacene instability.^{32,33} Using quadratic relationship between number of rings and ASE values (Table 3) one estimates that the ASE will reach a maximum value of -157 kcal/mol near $x = 18$, i.e. octadecacene. The quadratic model further predicts that ASE should rather (strangely) decrease beyond octadecacene becoming -14, zero and positive (anti-aromatic) for polyacene with 37, 38 and higher number of fused benzene rings respectively. This model contradicts with the Hückel's rule for higher PAH (above octadecacene), literature understanding on polyacenes, aromatic compounds and is likely to be an artifact/limitation of the quadratic model. Nevertheless, as mentioned earlier the quadratic regression model agrees with the experimental findings about instability of higher polyacenes in general and will be tested further in our future studies on aromaticity. At present our computational resources prevent us from further exploring this strange finding on still higher PAH. The logarithmic regression model (with lower correlation, Table 3) estimates a limiting value of 90 fused benzene rings (ASE = -224 kcal/mol) where differences in ASE falls below 0.5 kcal/mol (typical accuracy of thermochemical experiments). Unlike the quadratic model, logarithmic regression model doesn't contradict Hückel's rule, literature understanding on

polyacenes and aromatic compounds, nor predicts strange decrease in ASE or antiaromatic character of higher polyacene derivatives. A linear model based on this data has lower correlation than the quadratic model (better than logarithmic model), but incorrectly predicts ASE values to increase with number of fused rings.

Table 3. Polyacene ASE values are calculated using HoH schemes (Figure 4). ASE per ring and residuals from the predicted values based on the best fit quadratic relationships are shown.

Polyacene	# of rings (x)	ASE estimated with HoH Scheme	ASE per ring	Residuals for quadratic model	Residuals for Logarithmic model
Benzene	1	-34.71	-34.71	4.85	0.49
Naphthalene	2	-54.74	-27.37	-1.79	4.51
Anthracene	3	-68.72	-22.91	-3.19	6.07
Tetracene	4	-79.94	-19.98	-2.63	6.25
Pentacene	5	-89.67	-17.93	-1.39	5.60
Hexacene	6	-98.41	-16.40	0.04	4.25
Heptacene	7	-106.61	-15.23	1.20	2.32
Octacene	8	-114.46	-14.31	1.90	0.01
Nonacene	9	-122.00	-13.56	2.10	-2.63
Decacene	10	-129.31	-12.93	1.74	-5.67
Undecacene	11	-136.59	-12.42	0.59	-11.12
Dodecacene	12	-145.91	-12.16	-3.39	-10.26
ASE = 0.4027*x ² - 14.595*x - 25.37; R2 = 0.9945: Quadratic model					
ASE = -9.3595*x - 37.586, R2 = 0.9776: Linear model					
ASE = -44.4*ln(x) -24.453, R2 = 0.9673: Logarithmic model.					

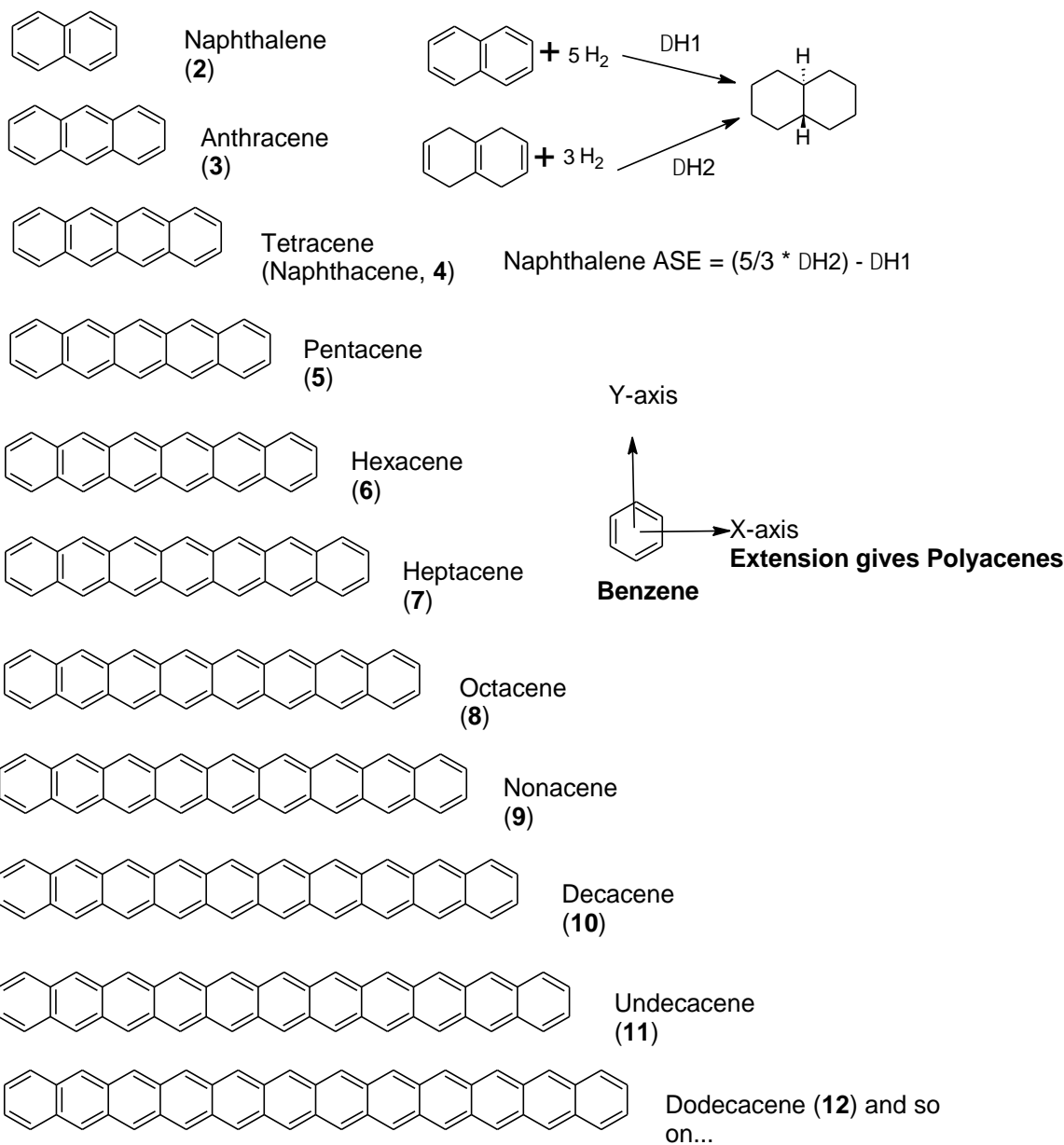


Figure 4. Polyacenes depicted as X-axis extension analogs of Benzene. Aromaticity in polyacenes is known to concentrate near the center and decrease along this series, but it is not known if it reaches a limiting value or not. Polyacene ASE was estimated with HoH schemes using differences in the enthalpy of hydrogenation reactions for the polyacene and corresponding unconjugated reference system (exemplified here for naphthalene). Reference compounds had trans configuration at the saturated chiral carbon atoms.

Thus extending benzene on the X-axis does not lead to a linear increase in ASE and stability. Rather according to quadratic regression model the ASE is likely to reach a maximum value of -157 kcal/mol in polyacenes containing 18 linearly fused benzene rings. While the logarithmic model predicts ASE to reach limiting value of -224 kcal/mol for polyacene with 90 fused benzene rings. Nevertheless, longer graphene models and

graphene itself (possessing simultaneous Y-axis extensions) are known to be stable. Thus it is very interesting to investigate the effect of Y-axis extensions of benzene on the ASE and aromaticity and ultimately that of graphene.

Benzene Y-axis extension gives
Pyrene-Vertacenes

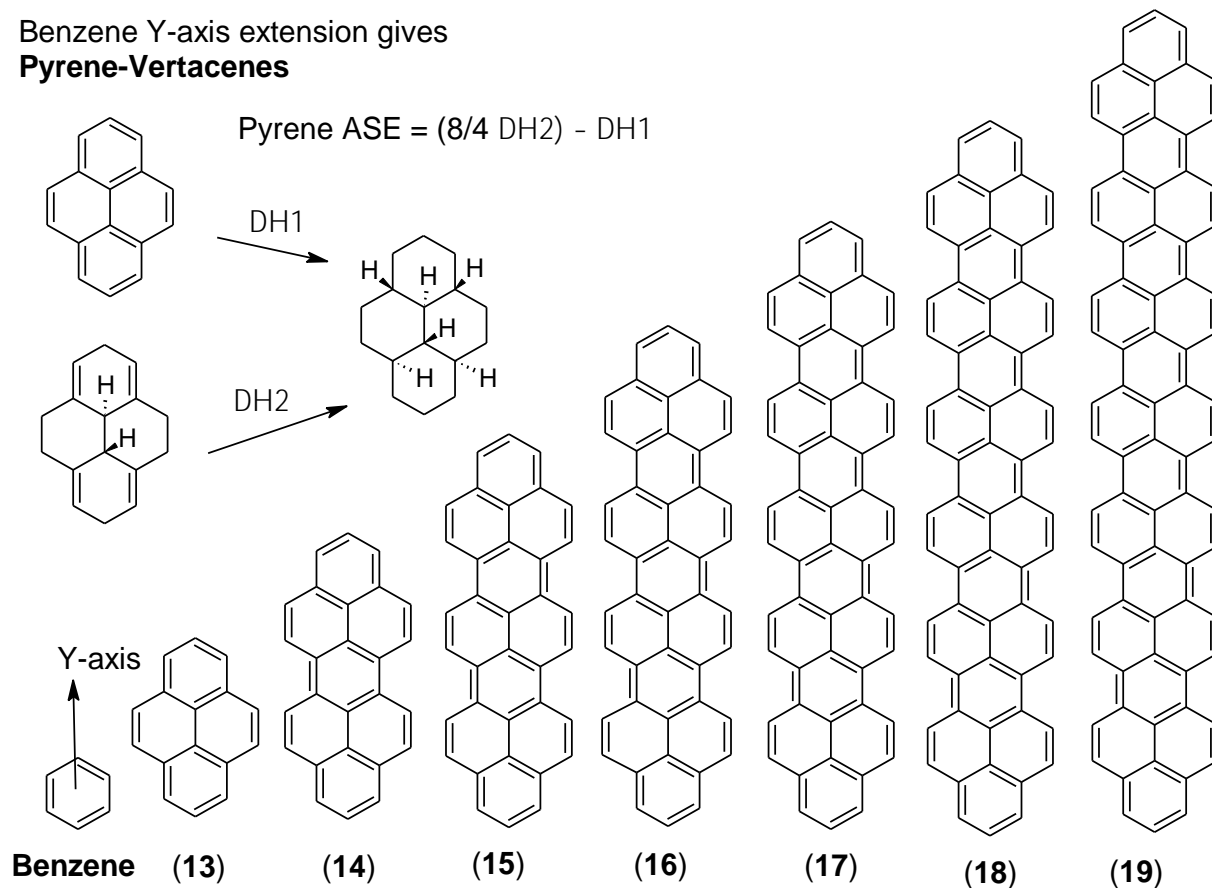


Figure 5. Benzene vertical (Y-axis) extension gives structures which are here called pyrene-vertacenes. Such analogous series of aromatic structures and trends in their aromaticity have not been considered in the literature so far. All chiral carbon atoms in partially saturated and fully saturated compounds had trans configuration and highest possible symmetry was employed during geometry optimization.

Figure 5 shows the structures of pyrene as a Y-axis extension of benzene and similar higher analogues, here called as pyrene-vertacenes (**13-19**) in analogy with polyacenes. The unconjugated unsaturated reference system and corresponding equation employed for estimating pyrene-vertacene ASE is exemplified in Figure 5. Table 4 shows the ASE values for pyrene-vertacenes (**14-19**) calculated with HoH schemes. Both the quadratic and linear regression models have similar correlations, residuals and thus fit the data in Table 4 equally well. But predictions for larger systems differ significantly between these models. The quadratic model predicts ASE to reach a maximum of 1,622 kcal/mol at around 32 layers of benzene in the pyrene-vertacenes.

Due to the natural behavior of quadratic models, ASE is predicted to decrease beyond this and become zero for pyrene-vertacenes containing 62-65 layers of benzene (refer Figure 5). The linear model, on the other hand, predicts no such limiting value and ASE is predicted to increase by ~ 92 kcal/mol for each higher analogue of pyrene-vertacene. The logarithmic model with lower correlation predicts a much larger limiting value of 627 benzene layer (and an ASE -1,948 kcal/mol). For larger pyrene-vertacenes expected differences in ASE with an increase in the size of the aromatic system are likely to fall below experimental error limits. Since the correlation for logarithmic model is lower (than quadratic, and linear models) and residuals are large, the predictions for larger pyrene-vertacenes should be considered as suggestive ones.

Table 4. ASE calculated at HF/6-31G(d) level using HoH schemes for Y-axis extensions of benzene ring.

# of Benzene Layers	Structures in Figure 5	ASE	Residuals for Quadratic model	Residuals for linear model	Residuals for logarithmic model
1	Benzene	-34.71	10.72	1.21	86.91
2	13 (pyrene)	-119.77	-6.85	8.57	-43.25
3	14	-210.41	-15.45	10.35	-78.51
4	15	-319.86	-1.83	-6.67	-58.38
5	16	-431.14	17.03	-25.52	-16.39
6	17	-495.69	-7.43	2.35	-8.45
7	18	-603.51	14.78	-13.04	51.50
8	19	-660.13	-10.80	22.76	66.67
$y = 1.7032x^2 - 107.75x + 82.06$, $R^2 = 0.997$: Quadratic model $y = -92.426x + 56.511$, $R^2 = 0.995$: Linear model $y = -310.5\ln(x) + 52.2$, $R^2 = 0.926$: Logarithmic model.					

3.5. ASE predictions for truncated graphene models and graphene

Graphene and truncated graphene models can be approximated as multiple layers of polyacenes fused with each other. Alternatively larger PAH systems may be considered as a combination of pyrene-vertacenes and different polyacenes (exemplified as A, B and C in Figure 6).

Figure 7 shows the structures for which ASE values were calculated using unsaturated unconjugated HoH schemes similar to those shown in Figure 4 and Figure 5 for polyacenes and pyrene-vertacenes. Table 6 shows ASE values calculated for truncated graphene models shown in Figure 6. Approximation A and B, show large % errors in estimation of ASE values. Approximation A consistently under predicts the ASE values, suggesting that it is not suitable for estimating ASE values resulting from Y-axis pyrene extensions. Thus large truncated graphene models, PAH and graphene cannot be approximated as simple layers of polyacenes kept one over the other. Approximation B includes rotated pyrene-vertacene structures, and overestimates ASE values. ASE values extrapolated using approximation C in Figure 6 have lowest % error from those calculated with HoH schemes. Inclusion of one pyrene-vertacene unit reduces the error in ASE prediction significantly. ASE values predicted using HoH schemes and approximation C are similar, $P(0.05) = 0.493$, while those predicted with approximation A and B are significantly different, $P = 0.038$ and 0.002 respectively. Therefore approximation C can be used to estimate ASE values for truncated graphene models and graphene.

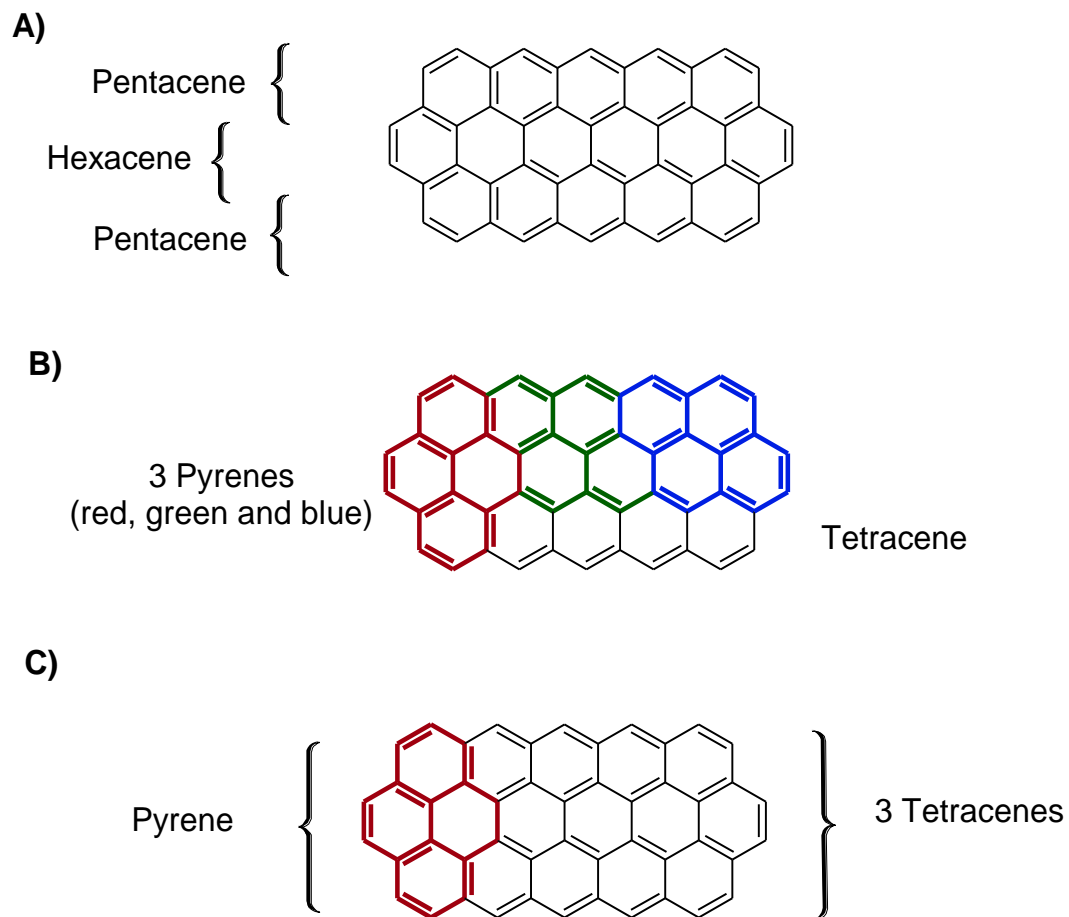


Figure 6. Truncated Graphene models approximated as A) Polyacene layers fused to each other, B) combination of maximum possible number of pyrene units (red, green and blue) and smaller polyacenes and C) One pyrene unit and laterally fused tetracenes.

Table 5. ASE values for truncated graphene models (shown in Figure 6) calculated using HoH schemes and predicted (extrapolated) using approximations shown in Figure 6.

Graphene models	Calculated ASE with HoH Schemes	ASE predicted with approximation models shown in Figure 6					
		A	% error	B	% error	C	% error
Naphthalene-pyrene	-254.82	-217.39	-17.22	-294.29	13.41	-297.98	14.48
Anthracene-pyrene	-311.11	-249.54	-24.67	-428.05	27.32	-337.16	7.73
Tetracene-pyrene	-363.71	-277.74	-30.95	-439.26	17.20	-369.32	1.52
Pentacene-pyrene	-414.03	-303.42	-36.45	-503.73	17.81	-388.77	-6.50
Hexacene-pyrene	-463.08	-327.67	-41.32	-577.50	19.81	-415.00	-11.59

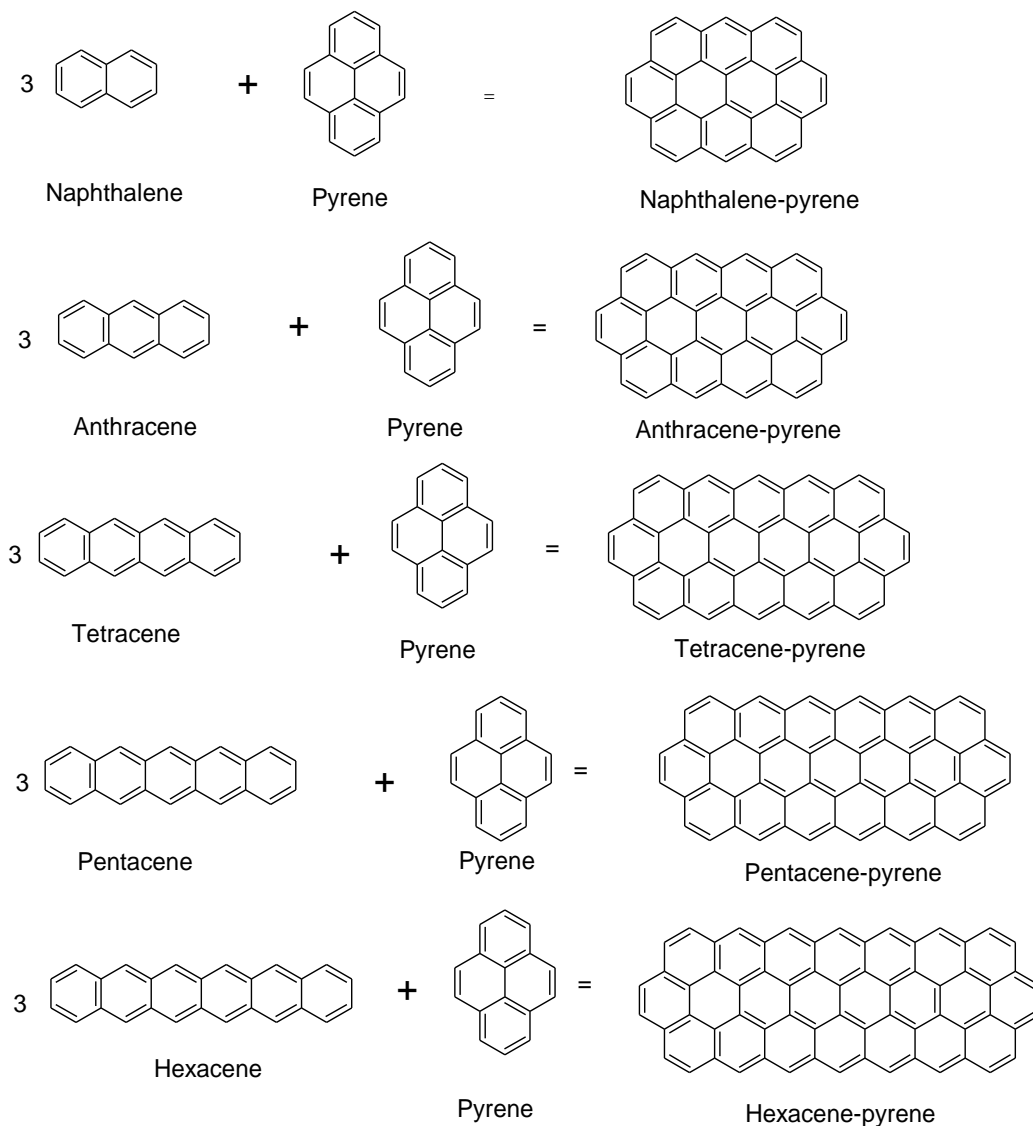


Figure 7. Truncated graphene models approximated as formed by the addition of polyacene and vertacene (pyrene) units (see C in Figure 6).

The ASE values for larger graphene models are therefore expected to depend on the relative components of X and Y-axis extensions present in the system. Thus ASE values for graphene models and graphene have been approximated using models discussed in section 3.4. A combination of quadratic models build for polyacene and pyrene-vertacenes suggests that a planar PAH with 37 fused benzene rings on the X-axis and about 62 pyrene-vertacene units on Y-axis will have little aromatic stabilization and is likely to be unstable. This compound is expected to have nanoparticle dimensions approximately 92.5 Å X 255 Å (9.25 nM X 25.5 nM, Table 6). (These estimates are based on the assumption that addition of each fused benzene ring

increases the size of the PAH by 2.5 Å on the X-axis and each additional pyrene unit on the Y-axis extends the molecule by approximately 4.11 Å). The logarithmic models predict the possibility of much larger PAH with maximum possible ASE value (Table 6). These are expected to contain 90 fused benzene rings on the X-axis and about 627 pyrene-vertacene units giving a nanometer sized graphene (~ 22.5 nM X 257.5 nM). Using approximation C in Figure 6, such a system is expected to have a large ASE value with an approximate upper bound of approximately -1,241,556 (-224*90 – 1948*627) kcal/mol.

Combinations of quadratic and logarithmic models predict lower limiting ASE values for comparable molecular sizes. Quadratic and logarithmic models based on polyacenes and pyrene-vertacenes respectively predicts a limiting ASE value of -1,947 kcal/mol for a PAH containing 37 fused benzene ring and 627 pyrene-vertacene units. Such a graphene molecule is expected to have dimensions ~ 92.5 nM X 257.5 nM (Table 6). While logarithmic and quadratic models for polyacene and pyrene-vertacenes respectively predicts a limiting ASE value of -224*90 = -20,160 kcal/mol for a polycyclic aromatic hydrocarbon containing 90 fused benzene ring and 62 pyrene-vertacene units and ~ 225 nM X 255 nM size. These estimates are also based on approximation C shown in Figure 6.

Since the linear models for polyacenes are unable to predict known decrease in ASE with increase in molecular size, they are expected to give unrealistically high predictions for graphene (Table 6). But the linear model (Table 4) for pyrene-vertacenes can be used to make extrapolations to graphene and suggest that Y-axis extensions are not likely cause a decrease in ASE with increase in molecular size (no limits on ASE values in Table 6). This hints that a graphene structure with arbitrarily large Y-axis extensions might be suitable for energy (hydrogen) storage applications. Likewise graphene structures with longer polyacene components may be suitable for electron transport and electronics applications. This finding is in concordance with an anisotropic behavior observed earlier in graphene and offers physical chemical insights into the phenomenon.⁵⁷

These predictions of ASE and molecular size are approximations for isolated PAH. Extrapolation to larger graphene models, derivatized graphene and graphene prepared using different methodologies and/or adsorbed on solid supports should be performed cautiously since such processes are known to significantly alter the electronic, physical and chemical properties.⁵⁸ Nevertheless these estimates for graphene sheet size are close to those found experimentally by Ishii et al⁴³ and Meyer et al.⁴⁴ Our results suggest that extension in either X or Y-axis (except for linear regression model) for planar PAH beyond these limits may not lead to an increase in ASE. Sheet bending (corrugated graphene), formation of spherical or cylindrical nano structures is known to lead to additional stabilization.^{59,60} These limiting ASE values and dimensions for planar PAH offer new physical insights and possible explanations for the absence of arbitrarily large (or infinite planar) graphene, formation of carbon nanotubes, and other structures reported earlier.^{44,61,58,52}

Table 6. Polyacenes, Vertacenes (pyrene-vertacenes) and graphene limiting ASE values, molecular size and dimensions predicted using models shown in Table 3 and Table 4.

Model/PAH	Limiting ASE (kcal/mol) and molecular size (nM)					
	Polyacenes	Vertacenes	Model	Extrapolated Graphene ASE and molecular dimension		
				Quadratic (Veratcenes)	Logarithmic (Vertacenes)	Linear (Vertacenes)
Quadratic	157 and 9.25	1,622 and 132	Quadratic (Polyacenes)	≈ 0 kcal/mol for PAH of dimensions 9.25 X 25.5	≈ -1,947 kcal/mol and 92.5 X 257.5	No limits on Y-axis extensions.
Logarithmic	224 and 22.5	1,948 and 257.5	Logarithmic (Polyacenes)	-20,160 kcal/mol for PAH of dimensions 225 X 255	≈ -1,241,556 kcal/mol for PAH of dimensions 22.5 X 257.	No limits on Y-axis extensions.
Linear	No limits (disagrees with experiments)	No limits	Linear (Polyacenes)	Potentially incorrect predictions		

4. Conclusions

Novel heat of hydrogenation (HoH) and isodesmic schemes have been proposed for the estimation of aromatic stabilization energy (ASE) in naphthalene. Comparison with values reported in the literature showed that schemes involving unconjugated unsaturated reference systems are best suited for ASE estimation. Conjugated and partially aromatic reference systems give reasonable and wrong ASE estimates respectively. Reference systems with unconjugated unsaturation at fused and terminal carbons (similar to row 15 in Table 1) offer advantages over isodesmic schemes and have been used for estimating ASE for polyacenes and Y-axis extensions of benzene (pyrene-vertacenes). These ASE estimates are in agreement with the known instability of higher polyacenes. Quadratic and logarithmic models show excellent correlations for the ASE data calculated using HoH schemes and correctly predict a decrease in ASE with increase in molecular size. For pyrene-vertacenes quadratic model predicts a limiting ASE value while an equivalent linear model predicts linear increase in ASE with molecular size. Simple approximations of truncated graphene models as combination of pyrene-vertacene and polyacene units make accurate ASE estimates for larger PAH. Graphene ASE extrapolations, reported for the first time, estimate limiting nanometer size ranges, offer new physical chemical (thermochemical) insights, and are consistent with recent reports on experimental graphene sizes. The predicted ASE and heats of hydrogenations represent first ever estimates for larger PAH, truncated graphene models and graphene. Predictions tentatively suggest that graphene based materials with larger polyacene fraction might be suitable for electronic applications. Whereas, for energy (hydrogen) storage applications graphene based materials with larger vertacene proportion may prove useful.

5. Conflicts of interest

There are no conflicts to declare.

6. References

- (1) von E. Doering, W.; Detert, F. L. CYCLOHEPTATRIENYLIUM OXIDE. *J. Am. Chem. Soc.* **1951**, *73* (2), 876–877.

- (2) Randić, M. Aromaticity and Conjugation. *J. Am. Chem. Soc.* **1977**, *99* (2), 444–450.
- (3) Kikuchi, S. A History of the Structural Theory of Benzene - The Aromatic Sextet Rule and Huckel's Rule. *J. Chem. Educ.* **1997**, *74* (2), 194.
- (4) Shaik, S. S.; Hiberty, P. C. When Does Electronic Delocalization Become a Driving Force of Molecular Shape and Stability? The "Aromatic" Sextet. *J. Am. Chem. Soc.* **1985**, *107* (11), 3089–3095.
- (5) Cyrański, M. K. Energetic Aspects of Cyclic Pi-Electron Delocalization: Evaluation of the Methods of Estimating Aromatic Stabilization Energies. *Chem. Rev.* **2005**, *105* (10), 3773–3811.
- (6) T. M. Krygowski Z. Czarnocki, G. Haßfelingerb and Alan R. Katritzky, M. K. C. Aromaticity: A Theoretical Concept of Immense Practical Importance. *Tetrahedron* **1999**, *56* (520), 1783–1796.
- (7) Cyran, M. K.; Krygowski, T. M.; Katritzky, A. R.; Rague, P. Von. To What Extent Can Aromaticity Be Defined Uniquely ? *J. Org. Chem.* **2002**, *67* (14), 1333–1338.
- (8) Krygowski, T. M.; Szatyłowicz, H. Aromaticity - What Does It Mean? *AIP Conf. Proc.* **2007**, *963* (2), 532–535.
- (9) Schleyer, P. V. R.; Jiao, H. What Is Aromaticity? *Pure Appl. Chem.* **1996**, *68* (2), 209–218.
- (10) Stanger, A. What Is . . . Aromaticity : A Critique of the Concept of Aromaticity — Can It Really Be Defined ? *Chem. Commun.* **2009**, 1939–1947.
- (11) Beckhaus, H.-D.; Faust, R.; Matzger, A. J.; Mohler, D. L.; Rogers, D. W.; Rüchardt, C.; Sawhney, A. K.; Verevkin, S. P.; Vollhardt, K. P. C.; Wolff, S. The Heat of Hydrogenation of (a) Cyclohexatriene. *J. Am. Chem. Soc.* **2000**, *122* (32), 7819–7820.
- (12) Turner, R. B.; Mallon, B. J.; Tichy, M.; Doering, W. V. E.; Roth, W. R.; Schroeder, G. Heats of Hydrogenation. X. Conjugative Interaction in Cyclic Dienes and Trienes. *J. Am. Chem. Soc.* **1973**, *95* (26), 8605–8610.
- (13) R, R. W.; Oliver, A.; Rolf, B.; Hans-Werner, L.; Roland, B. Die Berechnung von Resonanzenergien; Das MM2ERW-Kraftfeld. *Chem. Ber.* **2006**, *124* (11), 2499–2521.
- (14) Gershoni-Poranne, R.; Stanger, A. Magnetic Criteria of Aromaticity. *Chem. Soc. Rev.* **2015**, *44* (18), 6597–6615.
- (15) Martín, N.; Scott, L. T. Challenges in Aromaticity: 150 Years after Kekulé's Benzene. *Chem. Soc. Rev.* **2015**, *44* (18), 6397–6400.
- (16) Kruszewski, J.; Krygowski, T. M. Definition of Aromaticity Basing on the Harmonic Oscillator Model. *Tetrahedron Lett.* **1972**, *13* (36), 3839–3842.
- (17) Dixit, V. A.; Goundry, W. R. F.; Tomasi, S. CC/B-N Substitution in Five Membered Heterocycles. A Computational Analysis. *New J. Chem.* **2017**, *41* (9), 3619–3633.
- (18) Burley, S. K.; Petsko, G. A. Aromatic-Aromatic Interaction: A Mechanism of Protein Structure Stabilization. *Source Sci. New Ser.* **1985**, *229* (4708), 23–28.
- (19) Dougherty, D. A. Cation-Pi Interactions in Chemistry and Biology: A New View of Benzene, Phe, Tyr, and Trp. *Science (80-)*. **1996**, *271* (5246), 163–168.
- (20) Chen, W.; Duan, L.; Wang, L.; Zhu, D. Adsorption of Hydroxyl- and Amino-Substituted Aromatics to Carbon Nanotubes. *Environ. Sci. Technol.* **2008**, *42* (18), 6862–6868.
- (21) Radke, M. Application of Aromatic Compounds as Maturity Indicators in Source Rocks and Crude Oils. *Mar. Pet. Geol.* **1988**, *5* (3), 224–236.
- (22) Ritchie, T. J.; Macdonald, S. J. F. Physicochemical Descriptors of Aromatic Character and

- Their Use in Drug Discovery. *J. Med. Chem.* **2014**, *57* (17), 7206–7215.
- (23) CYSEWSKI, P. Application of Aromaticity Indices As Molecular Descriptors for Prediction of Optical Properties of 9,10-Anthraquinone Derivatives in Ethanol Solution. *J. Theor. Comput. Chem.* **2013**, *12* (06), 1350050.
- (24) Lovas, F. J.; McMahan, R. J.; Grabow, J.; Schnell, M.; Mack, J.; Scott, L. T.; Kuczkowski, R. L.; Chemie, P.; Lehrgebiet, A.; Uni, V.; et al. Interstellar Chemistry : A Strategy for Detecting Polycyclic Aromatic Hydrocarbons in Space. *J. Am. Chem. Soc.* **2005**, *127* (11), 4345–4349.
- (25) Choi, J.; Kim, K. H.; Yu, H.; Lee, C.; Kang, H.; Song, I.; Kim, Y.; Oh, J. H.; Kim, B. J. Importance of Electron Transport Ability in Naphthalene Diimide-Based Polymer Acceptors for High-Performance, Additive-Free, All-Polymer Solar Cells. *Chem. Mater.* **2015**, *27* (15), 5230–5237.
- (26) Sanctucci, K.; Shah, B. Association of Naphthalene with Acute Hemolytic Anemia. *Acad. Emerg. Med.* **2000**, *7* (1), 42–47.
- (27) Slayden, S. W.; Liebman, J. F. The Energetics of Aromatic Hydrocarbons: An Experimental Thermochemical Perspective. *Chem. Rev.* **2001**, *101* (5), 1541–1566.
- (28) Von Ragué Schleyer, P.; Puhlhofer, F. Recommendations for the Evaluation of Aromatic Stabilization Energies. *Org. Lett.* **2002**, *4* (17), 2873–2876.
- (29) Wheeler, S. E. Homodesmotic Reactions for Thermochemistry. *Wiley Interdiscip. Rev. Comput. Mol. Sci.* **2011**, *2* (2), 204–220.
- (30) Wheeler, S. E.; Houk, K. N.; Schleyer, P. v. R.; Allen, W. D. A Hierarchy of Homodesmotic Reactions for Thermochemistry. *J. Am. Chem. Soc.* **2009**, *131* (7), 2547–2560.
- (31) Schleyer, P. von R.; Manoharan, M.; Jiao, H.; Stahl, F. The Acenes: Is There a Relationship between Aromatic Stabilization and Reactivity? *Org. Lett.* **2001**, *3* (23), 3643–3646.
- (32) Mondal, R.; Tönshoff, C.; Khon, D.; Neckers, D. C.; Bettinger, H. F. Synthesis, Stability, and Photochemistry of Pentacene, Hexacene, and Heptacene: A Matrix Isolation Study. *J. Am. Chem. Soc.* **2009**, *131* (40), 14281–14289.
- (33) Einholz, R.; Fang, T.; Berger, R.; Grüninger, P.; Früh, A.; Chassé, T.; Fink, R. F.; Bettinger, H. F. Heptacene: Characterization in Solution, in the Solid State, and in Films. *J. Am. Chem. Soc.* **2017**, *139* (12), 4435–4442.
- (34) Kaur, I.; Jazdyk, M.; Stein, N. N.; Prusevich, P.; Miller, G. P. Design, Synthesis, and Characterization of a Persistent Nonacene Derivative. *J. Am. Chem. Soc.* **2010**, *132* (4), 1261–1263.
- (35) Stankovich, S.; Dikin, D. A.; Dommett, G. H. B.; Kohlhaas, K. M.; Zimney, E. J.; Stach, E. A.; Piner, R. D.; Nguyen, S. T.; Ruoff, R. S. Graphene-Based Composite Materials. *Nature* **2006**, *442* (7100), 282–286.
- (36) Chen, J.-H.; Jang, C.; Xiao, S.; Ishigami, M.; Fuhrer, M. S. Intrinsic and Extrinsic Performance Limits of Graphene Devices on SiO₂. *Nat. Nanotechnol.* **2008**, *3* (4), 206–209.
- (37) Novoselov, K. S.; Geim, A. K.; Morozov, S. V.; Jiang, D.; Zhang, Y.; Dubonos, S. V.; Grigorieva, I. V.; Firsov, A. A. Electric Field Effect in Atomically Thin Carbon Films. *Science (80-.)*. **2004**, *306* (5696), 666.
- (38) Allen, M. J.; Tung, V. C.; Kaner, R. B. Honeycomb Carbon: A Review of Graphene. *Chem. Rev.* **2010**, *110* (1), 132–145.

- (39) Popov, I. A.; Bozhenko, K. V.; Boldyrev, A. I. Is Graphene Aromatic? *Nano Res.* **2012**, *5* (2), 117–123.
- (40) Zdetsis, A. D.; Economou, E. N. A Pedestrian Approach to the Aromaticity of Graphene and Nanographene: Significance of Huckel's $(4n+2)\pi$ Electron Rule. *J. Phys. Chem. C* **2015**, *119* (29), 16991–17003.
- (41) Nishina, N.; Makino, M.; Aihara, J. Aromatic Character of Irregular-Shaped Nanographenes. *J. Phys. Chem. A* **2016**, *120* (15), 2431–2442.
- (42) Otero, N.; El-kelany, K. E.; Pouchan, C.; Rerat, M.; Karamanis, P. Establishing the Pivotal Role of Local Aromaticity in the Electronic Properties of Boron-Nitride Graphene Lateral Hybrids. *Phys. Chem. Chem. Phys.* **2016**, *18* (36), 25315–25328.
- (43) Ishii, T.; Kashihara, S.; Hoshikawa, Y.; Ozaki, J.; Kannari, N.; Takai, K.; Enoki, T.; Kyotani, T. A Quantitative Analysis of Carbon Edge Sites and an Estimation of Graphene Sheet Size in High-Temperature Treated, Non-Porous Carbons. *Carbon N. Y.* **2014**, *80*, 135–145.
- (44) Meyer, J. C.; Geim, A. K.; Katsnelson, M. I.; Novoselov, K. S.; Booth, T. J.; Roth, S. The Structure of Suspended Graphene Sheets. *Nature* **2007**, *446*, 60.
- (45) Cabria, I.; López, M. J.; Alonso, J. A. Enhancement of Hydrogen Physisorption on Graphene and Carbon Nanotubes by Li Doping. *J. Chem. Phys.* **2005**, *123* (20), 204721.
- (46) Elias, D. C.; Nair, R. R.; Mohiuddin, T. M. G.; Morozov, S. V.; Blake, P.; Halsall, M. P.; Ferrari, A. C.; Boukhvalov, D. W.; Katsnelson, M. I.; Geim, A. K.; et al. Control of Graphene Properties by Reversible Hydrogenation: Evidence for Graphane. *Science (80-.)*. **2009**, *323* (5914), 610.
- (47) Schmidt, M.; Baldridge, K.; Boatz, J.; Elbert, S.; Gordon, M.; Jensen, J.; Shiro, K.; Nikita, M.; Nguyen, K.; Shujun, S.; et al. General Atomic and Molecular Electronic Structure System. *J. Comput. Chem.* **2018**, *14* (11), 1347–1363.
- (48) Gordon, M. S.; Schmidt, M. W. Chapter 41 - Advances in Electronic Structure Theory: GAMESS a Decade Later. In *Theory and Applications of Computational Chemistry*; Dykstra, C. E., Frenking, G., Kim, K. S., Scuseria, G. E., Eds.; Elsevier: Amsterdam, 2005; pp 1167–1189.
- (49) Bode, B. M.; Gordon, M. S. Macmolplt: A Graphical User Interface for GAMESS. *J. Mol. Graph. Model.* **1998**, *16* (3), 133–138.
- (50) Jeffrey P. Merrick; Damian Moran, A.; Radom, L. An Evaluation of Harmonic Vibrational Frequency Scale Factors. *J. Phys. Chem. A* **2007**, *111*, 11683–11700.
- (51) Dixit, V. A.; Goundry, W. R. F.; Tomasi, S. C=C/B–N Substitution in Five Membered Heterocycles. A Computational Analysis. *New J. Chem.* **2017**, *41* (9), 3619–3633.
- (52) Karadakov, P. B. Do Large Polycyclic Aromatic Hydrocarbons and Graphene Bend? How Popular Theoretical Methods Complicate Finding the Answer to This Question. *Chem. Phys. Lett.* **2016**, *646*, 190–196.
- (53) Yu, J.; Sumathi, R.; Green, W. H. Accurate and Efficient Method for Predicting Thermochemistry of Polycyclic Aromatic Hydrocarbons– Bond-Centered Group Additivity. *J. Am. Chem. Soc.* **2004**, *126* (39), 12685–12700.
- (54) Morrison, RT; Boyd, R. *Organic Chemistry*, Sixth Edit.; Prentice Hall: Boston, 1983.
- (55) Schleyer, P. von R.; Pühlhofer, F. Recommendations for the Evaluation of Aromatic Stabilization Energies. *Org. Lett.* **2002**, *4* (17), 2873–2876.
- (56) E, W. S. Homodesmotic Reactions for Thermochemistry. *Wiley Interdiscip. Rev. Comput.*

- Mol. Sci.* **2011**, *2* (2), 204–220.
- (57) Park, C.-H.; Yang, L.; Son, Y.-W.; Cohen, M. L.; Louie, S. G. Anisotropic Behaviours of Massless Dirac Fermions in Graphene under Periodic Potentials. *Nat. Phys.* **2008**, *4*, 213.
- (58) Bhuyan, M. S. A.; Uddin, M. N.; Islam, M. M.; Bipasha, F. A.; Hossain, S. S. Synthesis of Graphene. *Int. Nano Lett.* **2016**, *6* (2), 65–83.
- (59) Linert, W.; Lukovits, I. Aromaticity of Carbon Nanotubes. *J. Chem. Inf. Model.* **2007**, *47* (3), 887–890.
- (60) Chen, Z.; King, R. B. Spherical Aromaticity: Recent Work on Fullerenes, Polyhedral Boranes, and Related Structures. *Chem. Rev.* **2005**, *105* (10), 3613–3642.
- (61) Jiang, J.; Li, Y.; Gao, C.; Kim, N. D.; Fan, X.; Wang, G.; Peng, Z.; Hauge, R. H.; Tour, J. M. Growing Carbon Nanotubes from Both Sides of Graphene. *ACS Appl. Mater. Interfaces* **2016**, *8* (11), 7356–7362.